



Comparison of adsorbent materials for herbicide diuron removal from water

Stefano Salvestrini^{a,*}, Jelena Jovanovic^b, Borivoj Adnadjevic^b

^aDepartment of Environmental, Biological and Pharmaceutical Sciences and Technologies, Second University of Naples, via Vivaldi 43, Caserta 81100, Italy, Tel. +39 0823274639; Fax: +39 0823274605; email: stefano.salvestrini@unina2.it

^bFaculty of Physical Chemistry, University of Belgrade, Studentski trg 12-16, Belgrade 11001, R. Serbia

Received 8 May 2015; Accepted 10 March 2016

ABSTRACT

Diuron herbicide is a persistent and frequently detected compound in surface and groundwater. In this work, a comparative study of the performance of four types of adsorbent (two precipitated silica, zeolite Y and carbon molecular sieves (CMS)) for removing diuron from water was carried out. Precipitated silica samples were obtained by controlled precipitation of SiO₂ with sulphuric acid from water glass; zeolite Y was synthesized by a microwave-assisted hydrothermal method; CMS were synthesized by the method of controlled pyrolysis of wheat straw and chemical vapour deposition of organic matter. It was found that adsorption isotherms for precipitated silica and zeolite type Y are of linear shape, whereas the one for CMS exhibits at low concentrations a concave shape followed by an inflection point which suggests cooperative adsorption and the formation of adsorbate multilayers. CMS adsorbent showed the highest adsorption capacity and this was likely due to its high hydrophobicity. Temperature has a negligible effect on precipitated silica and zeolite Y while it strongly affects adsorption properties of CMS. Adsorption is not thermodynamically favoured at high temperature. An unexpected decrease in the rate of adsorption was observed with increase in temperature. This is possibly related to the different adsorption behaviour of diuron conformers and aggregates.

Keywords: Diuron; Adsorption; Carbon molecular sieves; Precipitated silica; Zeolite Y

1. Introduction

Herbicides are extensively used throughout the world to control weeds in order to increase the agricultural production. Conventionally, for more effective use, herbicides are applied in excess in the fields causing serious problems for the environment and human health. During their application they may

affect non-target organisms and can lead to loss of biodiversity. Depending on their chemical properties, herbicides can be easily transformed through biotic/abiotic degradation pathways or persist in soil in an adsorbate state and leach to groundwater and surface water.

Among herbicides, diuron is one of the most widely used [1]. Diuron belongs to the group of phenylurea compounds and acts as a non-selective herbicide for both pre-emergent and post-emergent

*Corresponding author.

Presented at EuroMed 2015: Desalination for Clean Water and Energy Palermo, Italy, 10–14 May 2015.
Organized by the European Desalination Society.

weed control on crop or non-crop sites [2,3] and is a persistent and frequently detected compound in surface and groundwater [4,5].

Although diuron is mainly degraded by microorganisms, its chemical degradation is important for human health issues because it leads to the formation of 3,4-dichloro aniline [6–10] which turns out to be more harmful than the parent compound. Organic matter plays an important role in the adsorption of diuron on soil [11–13]. Soil organic matter may also act as an efficient catalyst of the abiotic degradation of diuron. This catalytic effect is due to carboxylic and phenol groups which can promote hydrolysis of the herbicide [6,9,10].

Among the most representative technologies aimed to remove diuron from water, we can mention oxidation [14], nanofiltration [15], photodegradation coupled with biodegradation [16] and adsorption. Adsorption is one of the water purification technologies most studied because it is a simple and relatively low-cost solution [17] and generally produces a high-quality treated effluent [18]. It involves the concentration of water pollutants on the surface of an adsorbent that can be sent to landfills or regenerated (e.g. by thermal treatment) after its use [19]. Over the years, several materials have been tested for the adsorption of diuron including aluminosilicate minerals [20,21] and carbon-based materials. Among the latter, we can mention for example multi-walled carbon nanotubes [22], activated carbon fibre and cloth [23,24] and granular activated carbon [24,25].

With the aim to find suitable materials and best operational conditions for diuron removal from water, in this work, a comparative study of the performance of four types of adsorbent (two precipitated silica, zeolite Y and carbon molecular sieves (CMS)) was carried out. In order to gain insight into adsorption mechanism, particular attention is paid to the effect of temperature on the equilibrium position and on the rate of the process.

2. Materials and methods

2.1. Reagents

Water glass and sodium aluminate were purchased from Factory of Alumina, Zvornik, BIH. Sodium hydroxide was supplied by Zorka Pharma, Sabac, R. Serbia. Sample of wheat straw was obtained from a local producer in R. Serbia. Benzene was purchased by Acros Organics, Belgium. N_2 was supplied by Messer, R. Serbia. All other chemicals, including diuron and methylene blue, were supplied by Sigma Aldrich, Germany.

2.2. Adsorbents

The adsorbent materials were synthesized according to the original procedure developed by Adnadjević and co-workers [26].

The samples of adsorbents based on SiO_2 (denoted as I1 and I2) were synthesized by applying the method of controlled precipitation. Water glass (360 g/L) and sulphuric acid were simultaneously dosed in separated steams during 60 min in a fixed volume of water glass (having SiO_2 concentration of 50 g/L) preheated at $T = 80^\circ C$. The formed reaction mixture was left to age during 15 min. After ageing, simultaneously introducing of water glass and sulphuric acid was continued for a further 30 min. The precipitated SiO_2 was separated from the mother liquid by filtration. The cake was rinsed with hot water and subsequently dried at $110^\circ C$. The solid products were ground to fine particles using mortar and pestle.

Zeolite type Y (denoted as I3) was synthesized by applying the method of crystallization from an amorphous mixture by using seed. Crystallization seed (molar ratio: 15 Na_2O : Al_2O_3 : 14 $SiO_2 \times 350 H_2O$) was obtained by mixing solution of water glass and sodium aluminate, at ambient temperature. The seed was aged 24 h at ambient temperature before use. Afterwards, the seed was introduced into the amorphous mixture (molar ratio: 4.5 Na_2O : Al_2O_3 : 10 $SiO_2 \times 180 H_2O$) obtained by mixing water glass and sodium aluminate preheated at $100^\circ C$. Reaction mixture was left to crystallize at $100^\circ C$ during next 4 h. The crystallized SiO_2 was separated from the mother liquid by filtration. The cake was rinsed with hot water and subsequently dried at $110^\circ C$. The solid products were ground to fine particles using mortar and pestle.

CMS were synthesized by the method of controlled pyrolysis of wheat straw and chemical vapor deposition of organic matter. Sample of wheat straw was obtained from a local producer in Serbia. The sample was dried, ground and sieved. The sieved sample of wheat straw was mixed with microwave susceptor (5% wt) and pyrolysed under N_2 flow in a microwave device (Discover, CEM Corporation, Matthews, North Carolina, USA) using power of 300 W at $800^\circ C$ during 10 min. The solid pyrolytic residue (63%) was cooled to ambient temperature under N_2 . The solid pyrolytic residue was firstly treated with 1 M HCl in order to remove microwave susceptor and metal's residuals. The obtained residual was rinsed with water and treated with 5 M NaOH in order to remove SiO_2 . This residual was again rinsed with water and dried at $120^\circ C$. Chemical vapour deposition was carried out in stainless steel reactor (diameter 2 cm, length 20 cm)

equipped with a vertical tubular furnace. The sample (5 g) was heated up to 800°C in nitrogen stream. Deposition was carried out with 30% benzene in N₂ during 45 min. The obtained sample was cooled down in N₂.

The moisture content determination was based on the weight loss after the thermal treatment of sample during 2 h at 120°C. The SiO₂ content was determined by measuring the weight loss of the sample (previously dissolved with HF) due to SiF₄ evaporation. Degree of crystallinity was determined by X-ray diffraction analyses. Degree of hydrophobicity (DH%) was determined according to the procedure previously described [27,28] measuring the ability of the material to adsorb non-polar substances (e.g. toluene) from the aqueous solution and it is given by the relation:

$$\text{DH}(\%) = \frac{X_{\text{toluene}}}{X_{\text{water}}} \times 100 \quad (1)$$

where X_{toluene} and X_{water} are the toluene and water adsorption capacity (g/g), respectively. The texture properties of the used adsorbent materials were determined using the adsorption–desorption N₂ isotherms. The BET surface area was measured from the adsorption isotherms by applying the Brunauer–Emmett–Teller equation. The total pore volume (V_p) was obtained at a relative pressure of 0.99. Micropore volume (V_{mp}) was determined based on T curve. The measurements were performed using a Micrometrics ASAP 2010 volumetric adsorption apparatus.

2.3. Adsorption experiments

One mL aliquots of diuron in deionized water, concentration range 1.7–17 mg L⁻¹, were added to 10 mg of each adsorbent in 1.5 mL Eppendorf tubes and kept at 10, 20, 30 or 40°C on a shaker at one oscillation per second. At programmed times, samples were centrifuged at 13,000 rpm for 15 min and analysed by HPLC on a Waters system, consisting of a 515 HPLC Pump and a 2487 dual λ Absorbance Detector, equipped with a C18 reversed phase column (3.9 × 150 mm). Diuron was eluted by a linear gradient of acetonitrile in water (50:50) in 8 min, flow rate 1 mL min⁻¹, $\lambda = 248$ nm.

Adsorption experiments on methylene blue were carried out at 20°C by adding 14 mL of methylene blue aqueous solution (1.25–12.5 mg L⁻¹) to 10 mg of each adsorbent. The samples were kept in polypropylene tubes under stirring and, at programmed times, centrifuged and analysed by spectrophotometric

method at 665 nm using a Lambda 40 Perkin Elmer spectrophotometer.

2.4. Kinetic data modelling

Kinetic adsorption data were modelled using the classical pseudo-first and pseudo-second order models. According to the pseudo-first model [29], the sorption rate is proportional to the difference of the amount sorbed at equilibrium (q_e) and at time t (q):

$$q = q_e(1 - e^{-k_1 t}) \quad (2)$$

where k_1 (h⁻¹) represents the pseudo-first kinetic rate constant.

The pseudo-second order model [30] assumes the rate of adsorption to be proportional to the second power of the difference in the amount of adsorbed solute at the and at time t , as given by:

$$q = \frac{q_e^2 k_2 t}{1 + q_e k_2 t} \quad (3)$$

where k_2 (kg mol⁻¹ h⁻¹) is the pseudo-second order kinetic constant.

2.5. Equilibrium data modelling

Sorption equilibrium data were analysed using a $\ln(q_e/C_e)$ vs. q_e plot or, where appropriate, by following the linear model:

$$q_e = K_d C \quad (4)$$

where C_e (mol L⁻¹) is the diuron concentration in the water phase at equilibrium, q_e is the amount of adsorbed solute (mol kg⁻¹) at the equilibrium whereas K_d (L kg⁻¹) is the adsorbate distribution coefficient between adsorbent and solution.

3. Results and discussion

The basic physicochemical properties of the employed adsorbents are given in Table 1.

As can be seen, the used adsorbents largely differ in their physicochemical properties. CMS, I1 and I2 are amorphous whereas I3 is crystalline. CMS is hydrophobic while the others are hydrophilic. I1 and I2 consist almost exclusively of SiO₂ and contain appreciable amounts of H₂O in contrast to CMS which does not contain neither SiO₂ nor H₂O.

Table 1
Basic physicochemical properties of the adsorbents used

| Physicochemical property | CMS | I1 | I2 | I3 |
|--|---------|------|------|-------|
| Degree of crystallinity (%) | 0 | 0 | 0 | 100 |
| SiO ₂ (%) | 0 | 99 | 99 | 72.5 |
| H ₂ O (%) | 0.01 | 6 | 6 | 1 |
| Specific surface area BET (SP) (m ² /g) | 890 | 175 | 130 | 700 |
| Pore volume (V _p) (cm ³ /g) | 0.5 | 1.84 | 1.10 | 0.39 |
| Micropore volume (V _{mp}) (cm ³ /g) | 0.39 | 0 | 0 | 0.034 |
| Diameter of granules (mm) | 1.6–3.4 | 0.2 | 0.2 | 0.2 |
| Degree of hydrophobicity (%) | 97 | 0 | 0 | 0 |

The texture properties of the used adsorbents are mutually different and vary within a wide range of values: specific surface area from 130 to 890 (m²/g); V_p from 0.39 to 1.84 cm³/g; V_{mp} from 0 to 0.39 cm³/g.

The adsorption isotherms of diuron on the four selected materials at T = 20 °C are reported in Fig. 1.

The isotherms of diuron onto I1, I2 and I3 show a linear trend (C-shape, according to the classification of Giles [31]) indicating that they are far from the saturation level and hence that the adsorbents exhibit constant affinity for diuron in the whole range of concentration explored. In line with these considerations, the adsorption data of I1, I2 and I3 were modelled using a linear model (see Materials and Methods section for details). The results of the fitting procedure are reported in Fig. 1 and Table 2.

On the contrary to that, the isotherm of diuron onto CMS displays an inflection point (L₄-shape) that

may indicate, in agreement with previous reports [21,25], cooperative adsorption of diuron and the formation of multilayers. Such complex adsorption behaviour cannot be taken into account by simple models such as the Langmuir model. In this case, to evaluate the thermodynamic parameters of the adsorption process, one can use the equilibrium constant K_C defined by:

$$K_C = \left(\frac{q_e}{C_e} \right)_{C_e \rightarrow 0} \quad (5)$$

Values of K_C were calculated from the intercept on the ordinate of the plot ln(q_e/C_e) against q_e [32]. This method presupposes that at low concentration (C_e → 0) the adsorption isotherm is a straight line, hence simulating a partitioning process. The results of this procedure are reported in Table 2.

The difference in adsorption capacity between I1, I2 and I3 can be evaluated in terms of texture properties of the adsorbents. More specifically, as can be seen from Tables 1 and 2, adsorption capacity increases with the increase of the pore volume values (V_p) suggesting that V_p has a dominant influence on the adsorption of diuron.

Significantly higher adsorption capacity of CMS in comparison to the other adsorbents used may be explained as a consequence of its high hydrophobicity. This is in agreement with soil adsorption studies of diuron reported in literature which indicate that the uptake of this pesticide primarily occurs via hydrophobic interactions on the soil organic fraction (hydrophobic fraction), with hydrophilic phase (e.g. clay minerals) playing a negligible role [9,11,13,33].

To further corroborate the hypothesis that hydrophobic interactions play an important role in the adsorption process, we carried out some adsorption experiments with methylene blue. Methylene blue (cationic dye) was chosen for its water solubility significantly higher than that of diuron (about 10³ times

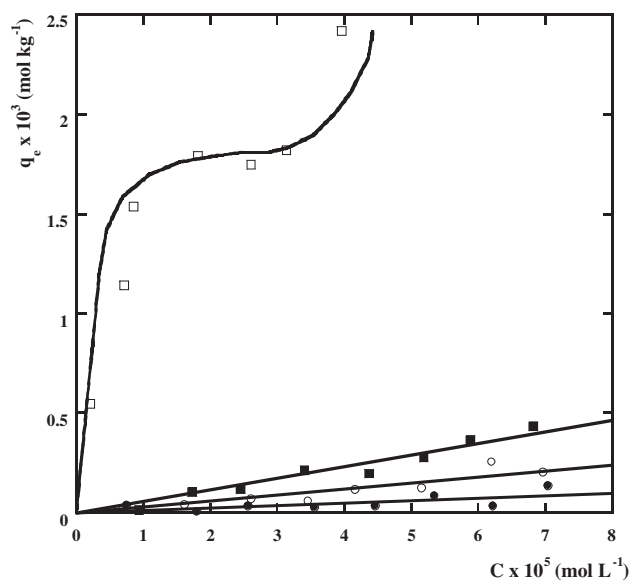


Fig. 1. Adsorption isotherms of diuron onto CMS (□), I1 (■) I2 (○) and I3 (●); T = 20 °C.

Table 2
Thermodynamic parameters for diuron adsorption

| Adsorbent | T (K) | K_C (L mol ⁻¹) | K_d (L kg ⁻¹) | ΔH° (kJ mol ⁻¹) | ΔS° (J K ⁻¹ mol ⁻¹) |
|-----------|---------|------------------------------|-----------------------------|--|---|
| CMS | 283 | 590 ± 310 | | -24 ± 5 | -33 ± 17 |
| | 293 | 469 ± 250 | | | |
| | 303 | 257 ± 95 | | | |
| | 313 | 240 ± 111 | | | |
| I1 | 293 | | 5.8 ± 0.3 | | |
| I2 | 293 | | 3.0 ± 0.3 | | |
| I3 | 293 | | 1.2 ± 0.2 | | |

higher). The results of these experiments are reported in Fig. 2.

It is interesting to observe that methylene blue exhibits an opposite behaviour with respect to diuron. Higher adsorbed amounts of methylene blue are obtained using I1, I2 and I3 (hydrophilic materials), whereas very low adsorption capacity is observed for CMS. This could be partially explained by the fact that methylene blue could not have the ability to enter all the adsorbent pores accessible to diuron (for steric reasons). Nevertheless, it is quite evident from the results that the adsorption behaviour of the two compounds, given their different nature, is also influenced by the different hydrophobic character of the adsorbents.

As regards the effect of temperature, we found that temperature does not lead to significant changes in the adsorption of diuron onto I1, I2 and I3, in agreement with the low affinity of the herbicide for these adsorbents. In fact, adsorption data obtained at 20 and

40 °C for the three adsorbents overlap within the experimental precision of the measurements (data not shown).

In contrast, concerning the adsorption of diuron onto CMS, it was found that temperature strongly affects the adsorbate–adsorbent interactions both from the thermodynamic and kinetic point of view. These aspects are extensively discussed below.

The effect of temperature on the adsorption equilibrium is shown in Fig. 3. Although the experimental data are scattered, it is evident that there is a significant increase of diuron uptake with the temperature. In addition, some isotherms display an inflection which suggests, as stated above, multilayer adsorption. The equilibrium constant K_C , calculated according to Eq. (4) and reported in Table 2, decreases with temperature indicating that adsorption is not thermodynamically favoured at high temperature (exothermic process). Increase of the adsorption capacity with

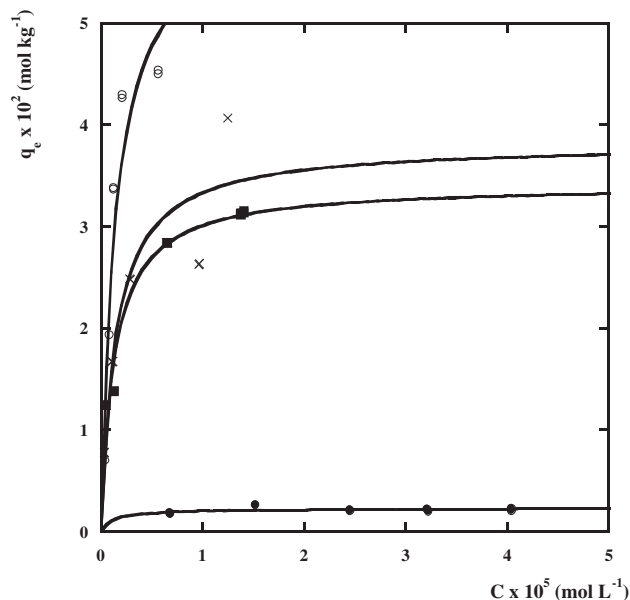


Fig. 2. Adsorption isotherms of methylene blue onto CMS (●), I1 (■) I2 (○) and I3 (x); $T = 20^\circ\text{C}$.

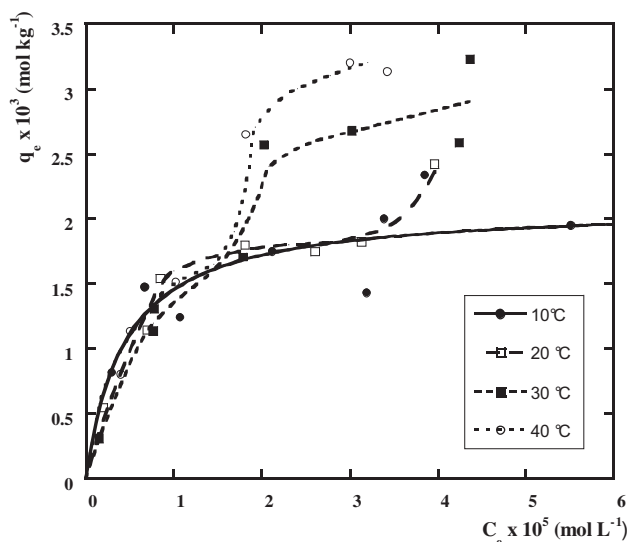


Fig. 3. Adsorption isotherms of diuron onto CMS at different temperatures: 10 °C (●), 20 °C (□), 30 °C (■), 40 °C (○).

temperature observed in Fig. 3, may be related to a better accessibility to CMS micropores, which in turn may depend on the increase of the adsorbent pore opening [34] and, as explained later, on the higher presence of planar conformers of diuron.

The standard enthalpy change (ΔH°) and the standard entropy change (ΔS°) of the process were calculated using the van't Hoff equation:

$$\ln K_C = -\frac{\Delta H^\circ}{R} \frac{1}{T} + \frac{\Delta S^\circ}{R} \quad (6)$$

Eq. (6) is valid under the assumption that both ΔH° and ΔS° change only slightly with the temperature. The plot $\ln(K_C)$ against $1/T$ should be linear, where the slope and the intercept are equal to $-\Delta H^\circ/R$ and $\Delta S^\circ/R$, respectively. Fig. 4 reports the van't Hoff plot, from which we calculated $\Delta H^\circ = -24 \text{ kJ mol}^{-1}$ and $\Delta S^\circ = -33 \text{ J K}^{-1} \text{ mol}^{-1}$.

The low value of ΔH° measured is within the range of values expected for physisorption [35] suggesting that diuron interacts with CMS by means of weak non-covalent forces (i.e. hydrophobic interactions).

To obtain further information on diuron-CMS interactions, we calculated the isosteric heat of adsorption (ΔH_{ist}) which represents the heat exchanged per mole during the adsorption of an infinitesimal amount of solute at constant coverage θ_e (with $\theta_e = q_e/q_m$) [32], using the following equation:

$$\ln C = \frac{\Delta H_{\text{ist}}}{R} \frac{1}{T} + \text{const} \quad (7)$$

where const is a dimensionless constant.

From plots of $\ln C$ vs. $1/T$ (see Fig. 5), values of ΔH_{ist} for different values of θ_e can be derived. The good linearity observed in the $\ln C$ vs. $1/T$ plot is a clear indication of the applicability of Eq. (7). The isosteric heat calculated is reported as a function of θ_e in

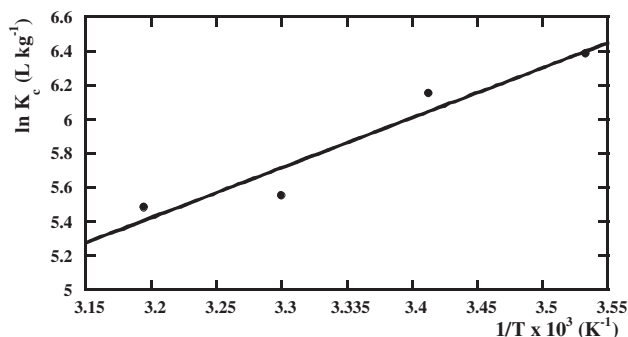


Fig. 4. Van't Hoff plot for diuron adsorption onto CMS.

Fig. 6. As can be seen, in the range of θ_e explored, ΔH_{ist} linearly increases with increase in θ_e .

These findings are quite interesting, as ΔH_{ist} normally decreases with increase in θ_e as a result of the non energetically homogeneity of the adsorbent surface [36]. When the adsorbent surface has different

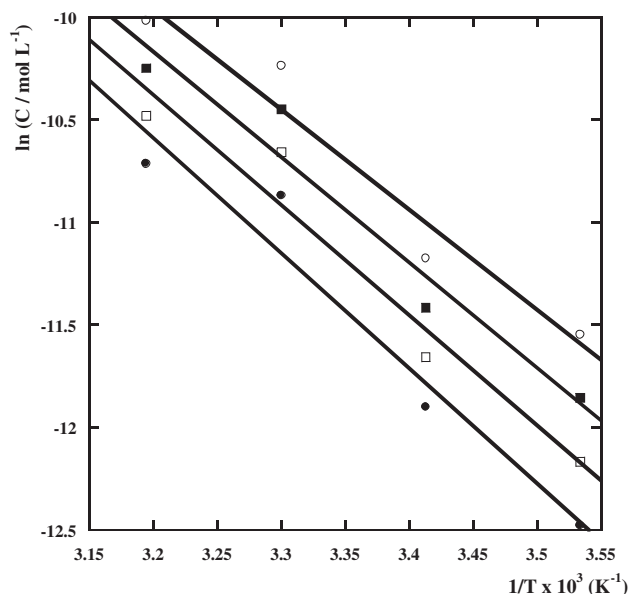


Fig. 5. Plots of the logarithms of the water equilibrium concentration (C) of diuron for four values of constant coverage (θ_e) vs. the reciprocal of the temperature; $\theta_e = 0.5$ (●) $\theta_e = 0.55$ (□) $\theta_e = 0.6$ (■) $\theta_e = 0.65$ (○).

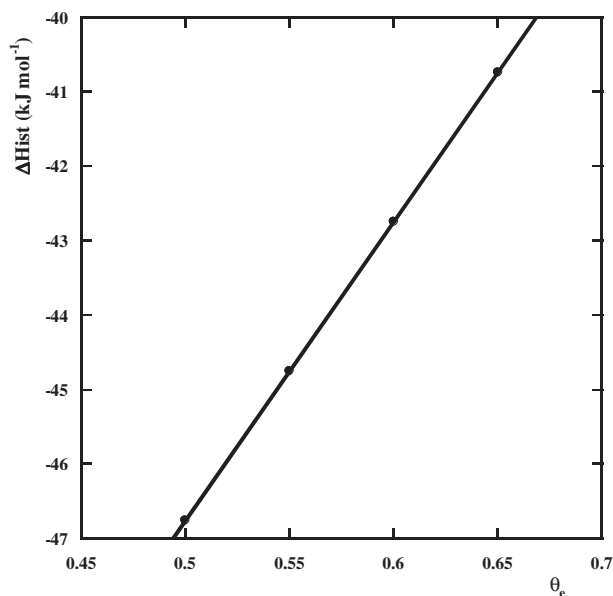


Fig. 6. Isosteric heat of adsorption of diuron (ΔH_{ist}) as a function of coverage (θ_e).

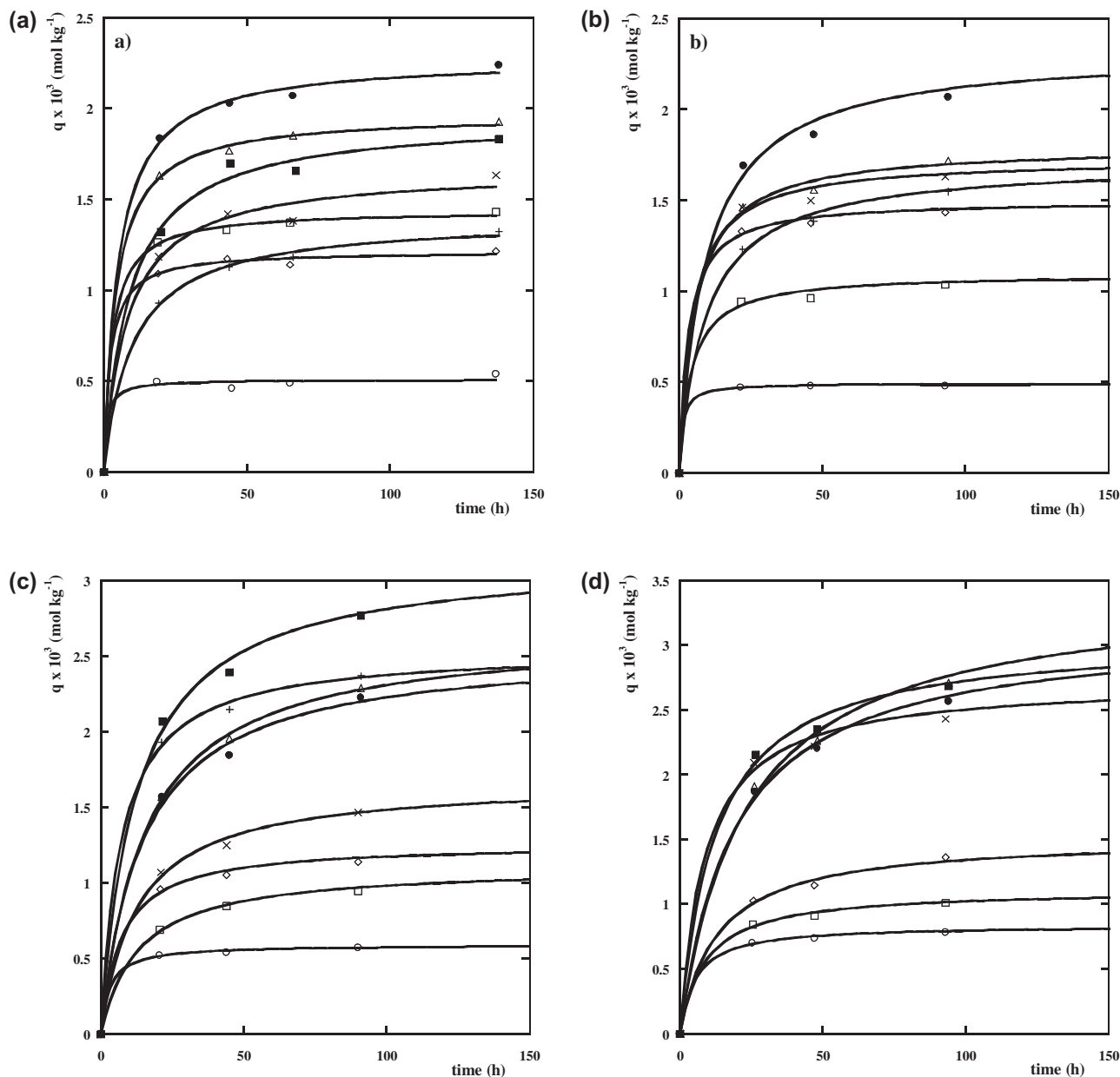


Fig. 7. (a–d) Kinetics of diuron adsorption onto CMS fitted by the pseudo-second order model at different temperatures and initial concentrations (C_0); (a) ($T = 10^\circ\text{C}$), (b) ($T = 20^\circ\text{C}$), (c) ($T = 30^\circ\text{C}$), (d) ($T = 40^\circ\text{C}$); $C_0 = 7.3 \times 10^{-6} \text{ M}$ (\circ); $C_0 = 1.7 \times 10^{-5} \text{ M}$ (\square); $C_0 = 2.6 \times 10^{-5} \text{ M}$ (\diamond); $C_0 = 3.6 \times 10^{-5} \text{ M}$ (\times); $C_0 = 4.5 \times 10^{-5} \text{ M}$ ($+$); $C_0 = 5.4 \times 10^{-5} \text{ M}$ (Δ); $C_0 = 6.4 \times 10^{-5} \text{ M}$ (\bullet); $C_0 = 7.3 \times 10^{-5} \text{ M}$ (\blacksquare).

energetic sites, molecules will adsorb preferentially at sites with the highest energy of adsorption and progressively go to lower energetic ones, resulting in a decrease of the heat of adsorption with the loading [37]. In contrast, we observed a linear increase of ΔH_{ist} with increase in θ_e which could be explained by the occurrence of positive interactions between adsorbate molecules during the adsorption process (cooperative adsorption). This hypothesis is consistent with the

results obtained by Al Bahri and co-workers [38] who showed that diuron adsorbs onto activated carbon via a cooperative mechanism.

The examination of kinetics may give some insight into the adsorption mechanism. The adsorption kinetics of diuron onto CMS at different initial concentrations and temperatures are displayed in Figs. 7(a)–(d). As can be seen, after a fast uptake during the first hours of the experiments, adsorption proceeds slower

until the equilibrium is reached (within about 2–6 d). Experimental data were modelled using the pseudo-first and the pseudo-second order equations. However, for the sake of brevity, we reported here only the results relative to the pseudo-second order model as it gave a better description of the data (curves in Fig. 7).

The results of the fitting procedure relative to an initial diuron concentration of $6.4 \times 10^{-5} \text{ mol L}^{-1}$ are shown, as an example, in Table 3. The model used gives a very good fit with the experimental data owing to the low error values of estimated parameters and high R^2 .

To explore the role of temperature on the rate of adsorption and thereby to gain information on the mechanism by which diuron interacts with CMS, the Arrhenius equation was used:

$$k_2 = Ae^{-E_a/RT} \quad (8)$$

In this equation k_2 is the pseudo-second order kinetic rate constant, A is the Arrhenius pre-exponential factor and E_a is the activation energy. A plot of $\ln k_2$ vs. $1/T$ (Arrhenius plot) should produce a straight line with slope and intercept equal to $-E_a/R$ and $\ln A$, respectively. The Arrhenius plot for the adsorption of diuron onto CMS is reported in Fig. 8.

It is very interesting to note from Table 3 and Fig. 8 that the observed kinetic rate constant (k_2) decreases with temperature resulting in an apparent negative activation energy. This clearly suggests that adsorption occurs via a multistep pathway.

It has been shown [39] that diuron can exist in aqueous solution in different conformations as a result of the formation of hydrogen bonds between solute and solvent which modify the shape and size of the herbicide. Moreover, diuron can be able to form aggregates in solution via intermolecular hydrogen bonding between acidic and basic functional groups [38]. Thus, the observed kinetics may depend on the different adsorption behaviour of diuron conformers

Table 3
Kinetic parameters for the adsorption of diuron onto CMS at different temperatures based on the pseudo-second order equation

| C_0 (mol L ⁻¹) | T (K) | k_2 (kg mol ⁻¹ h ⁻¹) | $q_e \times 10^5$ (mol kg ⁻¹) | R^2 |
|------------------------------|---------|---|---|-------|
| 6.4×10^{-5} | 283 | 89 ± 16 | 227 ± 4 | 0.999 |
| | 293 | 46 ± 11 | 233 ± 8 | 0.995 |
| | 303 | 27 ± 4 | 255 ± 7 | 0.997 |
| | 313 | 17 ± 2 | 313 ± 7 | 0.998 |

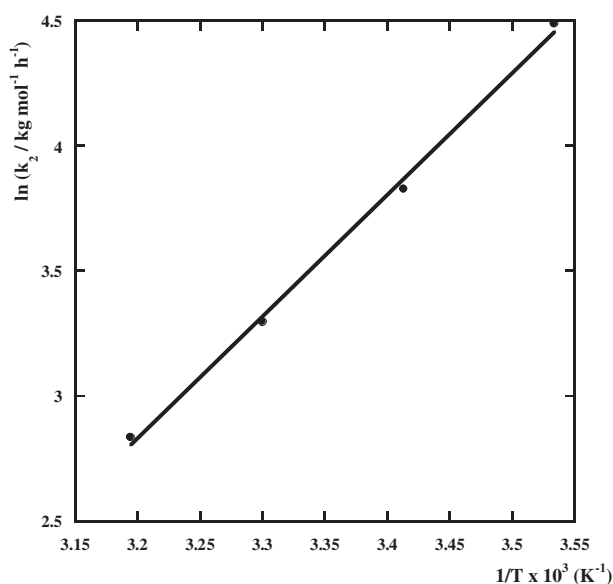


Fig. 8. Arrhenius plot for diuron adsorption onto CMS.

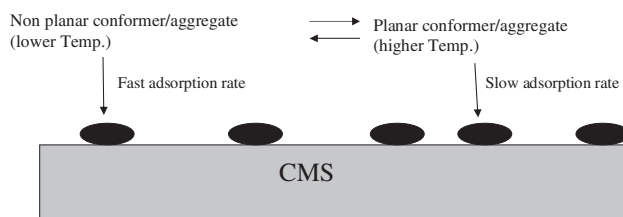


Fig. 9. Adsorption mechanism proposed for diuron adsorption onto CMS.

and aggregates. The most stable diuron conformers at lower temperature are non-planar [40], whereas with increase in temperature, hydrogen bonds become weaker thus leading to an higher presence of diuron in the planar conformation. Assuming that the uptake of planar conformer and of planar aggregates occurs with a slower rate, as temperature increases, conformational equilibrium shifts towards the planar conformer leading to a decrease in the observed adsorption rate and an apparent negative activation energy (Fig. 9).

4. Conclusions

In this work the adsorption behaviour of diuron onto four different adsorbents was examined. The adsorption capacity for diuron decreased in the sequence CMS >> I1 > I2 > I3 as a consequence of the hydrophobicity and the pore volume of the materials. It was found that temperature strongly affects

diuron adsorption onto CMS. The process is not thermodynamically favoured at high temperature. The observed adsorption rate decreases with temperature indicating that diuron adsorbs via a multistep mechanism which probably involves the onset of equilibrium between different diuron conformers and aggregates in the water phase.

References

- [1] R. Dragone, R. Cheng, G. Grasso, C. Frazzoli, Diuron in water: Functional toxicity and intracellular detoxification patterns of active concentrations assayed in tandem by a yeast-based probe, *Int. J. Environ. Res. Public Health* 12 (2015) 3731–3740.
- [2] S. Armenta, G. Quintás, A. Morales, S. Garrigues, M. de la Guardia, FTIR approaches for diuron determination in commercial pesticide formulations, *J. Agric. Food Chem.* 53 (2005) 5842–5847.
- [3] S. Kottuparambil, S. Lee, T. Han, Single and interactive effects of the antifouling booster herbicides diuron and Irgarol 1051 on photosynthesis in the marine cyanobacterium, *Arthrospira maxima*, *Toxicol. Environ. Health Sci.* 5 (2013) 71–81.
- [4] M. Thevenot, S. Dousset, Compost effect on diuron retention and transport in structured vineyard soils, *Pedosphere* 25 (2015) 25–36.
- [5] J.E. Brodie, F.J. Kroon, B. Schaffelke, E.C. Wolanski, S.E. Lewis, M.J. Devlin, I.C. Bohnet, Z.T. Bainbridge, J. Waterhouse, A.M. Davis, Terrestrial pollutant runoff to the Great Barrier Reef: An update of issues, priorities and management responses, *Mar. Pollut. Bull.* 65 (2012) 81–100.
- [6] S. Salvestrini, Diuron herbicide degradation catalyzed by low molecular weight humic acid-like compounds, *Environ. Chem. Lett.* 11 (2013) 359–363.
- [7] S. Salvestrini, P. Di Cerbo, S. Capasso, Kinetics and mechanism of hydrolysis of phenylureas, *J. Chem. Soc., Perkin Trans. 2* (2002) 1889–1893.
- [8] S. Salvestrini, P. Di Cerbo, S. Capasso, Kinetics of the chemical degradation of diuron, *Chemosphere* 48 (2002) 69–73.
- [9] S. Salvestrini, E. Coppola, S. Capasso, Determination of the microscopic rate constants for the hydrolysis of diuron in soil/water mixture, *Chemosphere* 55 (2004) 333–337.
- [10] S. Salvestrini, S. Capasso, P. Iovino, Catalytic effect of dissolved humic acids on the chemical degradation of phenylurea herbicides, *Pest Manage. Sci.* 64 (2008) 768–774.
- [11] S. Salvestrini, E. Coppola, S. Capasso, Sorption of diuron by soils and dissolved humic acids: Free energy interaction, *Fresen. Environ. Bull.* 13 (2004) 233–237.
- [12] Y. Liu, Z. Xu, X. Wu, W. Gui, G. Zhu, Adsorption and desorption behavior of herbicide diuron on various Chinese cultivated soils, *J. Hazard. Mater.* 178 (2010) 462–468.
- [13] P. Wang, A.A. Keller, Sorption and desorption of atrazine and diuron onto water dispersible soil primary size fractions, *Water Res.* 43 (2009) 1448–1456.
- [14] M. Carrier, M. Besson, C. Guillard, E. Gonze, Removal of herbicide diuron and thermal degradation products under catalytic wet air oxidation conditions, *Appl. Catal. B: Environ.* 91 (2009) 275–283.
- [15] Y. Wang, L. Shu, V. Jegatheesan, B. Gao, Removal and adsorption of diuron through nanofiltration membrane: The effects of ionic environment and operating pressures, *Sep. Purif. Technol.* 74 (2010) 236–241.
- [16] M.J. Farre, X. Domenech, J. Peral, Combined photo-Fenton and biological treatment for Diuron and Linuron removal from water containing humic acid, *J. Hazard. Mater.* 147 (2007) 167–174.
- [17] N.H. Mthombeni, S. Mbakop, M.S. Onyango, Magnetic zeolite-polymer composite as an adsorbent for the remediation of wastewaters containing vanadium, *Int. J. Environ. Sci. Dev.* 6 (2015) 602–605.
- [18] O.S. Bello, I.A. Bello, K.A. Adegoke, Adsorption of dyes using different types of sand: A review, *S. Afr. J. Chem.* 66 (2013) 117–129.
- [19] X. Peng, Z. Luan, H. Zhang, Montmorillonite–Cu(II)/Fe(III) oxides magnetic material as adsorbent for removal of humic acid and its thermal regeneration, *Chemosphere* 63 (2006) 300–306.
- [20] C. Maqueda, M. dos Santos Afonso, E. Morillo, R.M. Torres Sánchez, M. Perez-Sayago, T. Undabeytia, Adsorption of diuron on mechanically and thermally treated montmorillonite and sepiolite, *Appl. Clay Sci.* 72 (2013) 175–183.
- [21] O. Bouras, J.-C. Bollinger, M. Baudu, H. Khalaf, Adsorption of diuron and its degradation products from aqueous solution by surfactant-modified pillared clays, *Appl. Clay Sci.* 37 (2007) 240–250.
- [22] J. Deng, Y. Shao, N. Gao, Y. Deng, C. Tan, S. Zhou, X. Hu, Multiwalled carbon nanotubes as adsorbents for removal of herbicide diuron from aqueous solution, *Chem. Eng. J.* 193–194 (2012) 339–347.
- [23] M.A. Ángeles Fontecha-Cámara, M.V. López-Ramón, M.A. Álvarez-Merino, C. Moreno-Castilla, Temperature dependence of herbicide adsorption from aqueous solutions on activated carbon fiber and cloth, *Langmuir* 22 (2006) 9586–9590.
- [24] M.V. López-Ramón, M.A. Fontecha-Cámara, M.A. Álvarez-Merino, C. Moreno-Castilla, Removal of diuron and amitrole from water under static and dynamic conditions using activated carbons in form of fibers, cloth, and grains, *Water Res.* 41 (2007) 2865–2870.
- [25] M. Al Bahri, L. Calvo, M.A. Gilarranz, J.J. Rodriguez, Diuron multilayer adsorption on activated carbon from CO₂ activation of grape seeds, *Chem. Eng. Commun.* 203 (2016) 103–113, doi: 10.1080/00986445.2014.934447.
- [26] B. Adnadjević, A. Popović, J. Jovanović, Summary of achieved results in application of new catalytic processes in environmental protection, in: P. Putanov (Ed.), *New Challenges in Catalysis III*, Serbian Academy of Sciences and Art, Branch in Novi Sad, Novi Sad, 2002, pp. 119–135.
- [27] B. Adnadjević, J. Jovanović, S. Gajnov, Effect of different physicochemical properties of hydrophobic zeolites on the pervaporation properties of PDMS—Membranes, *J. Membr. Sci.* 136 (1997) 173–179.
- [28] J. Weitkamp, S. Ernst, E. Roland, G.F. Thiele, The modified hydrophobicity index as a novel method for characterizing the surface of titanium silicalites, *Stud. Surf. Sci. Catal.* 105 (1997) 763–770.

- [29] S. Lagergren, Zur theorie der sogenannten adsorption gelöster (About the Theory of So-Called Adsorption of Soluble Substance), K. Sven. Vetenskapsakad. Handl 24 (1898) 1–39.
- [30] Y.S. Ho, G. McKay, Pseudo-second order model for sorption processes, *Process Biochem.* 34 (1999) 451–465.
- [31] C.H. Giles, T.H. MacEwan, S.N. Nakhwa, D. Smith, *Studies in Adsorption. Part XI. A system of classification of solution adsorption isotherms and its use in diagnosis of adsorption mechanisms and in measurement of specific surface areas of solids*, *J. Chem. Soc.* (1960) 3973–3993.
- [32] S. Salvestrini, V. Leone, P. Iovino, S. Canzano, S. Capasso, Considerations about the correct evaluation of sorption thermodynamic parameters from equilibrium isotherms, *J. Chem. Thermodyn.* 68 (2014) 310–316.
- [33] V. Chaplain, A. Brault, D. Tessier, P. Défossez, Soil hydrophobicity: A contribution of diuron sorption experiments, *Eur. J. Soil Sci.* 59 (2008) 1202–1208.
- [34] R.E. Rogers, M. Ramurthy, G. Rodvelt, M. Mullen, *Coalbed Methane Principles and Practices*, Oktibbeha Publishing Co., Starkville, MS, 2007.
- [35] D.M. Ruthven, *Principles of Adsorption and Adsorption Processes*, Wiley, New York, NY, 1984.
- [36] S.M. Silva, K.A. Sampaio, R. Ceriani, R. Verhé, C. Stevens, W. De Greyt, A.J.A. Meirelles, Adsorption of carotenes and phosphorus from palm oil onto acid activated bleaching earth: Equilibrium, kinetics and thermodynamics, *J. Food Eng.* 118 (2013) 341–349.
- [37] D.D. Do, *Adsorption Analysis: Equilibria and Kinetics*, Imperial College Press, London, 1998.
- [38] M. Al Bahri, L. Calvo, J. Lemus, M.A. Gilarranz, J. Palomar, J.J. Rodriguez, Mechanistic understanding of the behavior of diuron in the adsorption from water onto activated carbon, *Chem. Eng. J.* 198–199 (2012) 346–354.
- [39] M. Fontecha-Cámara, M.V. López-Ramón, M.A. Álvarez-Merino, C. Moreno-Castilla, About the endothermic nature of the adsorption of the herbicide diuron from aqueous solutions on activated carbon fiber, *Carbon* 44 (2006) 2335–2338.
- [40] H.F. Dos Santos, P.J. O'Malley, W.B. De Almeida, Gas phase and water solution conformational analysis of the herbicide diuron (DCMU): An *ab initio* study, *Theor. Chem. Acc. Theory Comput. Model. (Theor. Chim. Acta)* 99 (1998) 301–311.